Vibration-buckling tests on heated composite plates

Álvarez, J. G.; Abramovich, Haim; Bisagni, Chiara

DOI
10.1016/j.jsv.2022.117145

Publication date
2022

Document Version
Final published version

Published in
Journal of Sound and Vibration

Journal of Sound and Vibration 536 (2022) 117145

Contents lists available at ScienceDirect

Journal of Sound and Vibration

journal homepage: www.elsevier.com/locate/jsvi

Vibration-buckling tests on heated composite plates

J.G. Álvarez [a], Haim Abramovich [b], Chiara Bisagni [a,*]

[a] Faculty of Aerospace Engineering, Delft University of Technology, Delft, the Netherlands
[b] Faculty of Aerospace Engineering, Technion, Israel Institute of Technology, Haifa, Israel

ARTICLE INFO

Keywords:
Thermal buckling
Vibration Correlation Technique
Carbon fibre
Thermal testing
Modal testing

ABSTRACT

This paper presents an experimental investigation on vibrations of heated composite plates leading to thermal buckling. The tests were performed considering two main goals: the application of the Vibration Correlation Technique for the detection of thermal buckling in composite plates; and the exploration of the frequency variations before and after the occurrence of a mode jump in post-buckling regime. Two test setups were used. The setups shared a low thermal expansion frame, while they differentiate on the type of heating source and mechanical boundary conditions. Two composite plates with layups $[30/-30/5/-5]_s$ and $[35/-35/10/-10]_s$ were tested. The plates were excited acoustically using a loudspeaker, and the vibration frequencies were monitored and stored using a laser vibrometer. Buckling temperatures were successfully detected using the Vibration Correlation Technique. Frequency changes, potentially related to the mode jumping, were also detected.

1. Introduction

Structural plates under heating can engage in typically stable, reversible post-buckled states and can operate under post-buckling conditions, as long as no material failure occurs. Structural situations reached after buckling may have potentially interesting applications, for instance, as a source for shape change [1]. An example of such deformed states are the so-called mode jumps, i.e. sudden changes in shape experienced in post-buckling, during which the buckled plates increase the number of half-waves as a response to load variations [2]. However, during buckling and post-buckling, plates experience variations in the vibration frequencies, which can have an impact on structural integrity. Plates intended to operate in those situations should have well-understood vibration behavior throughout all their operative ranges. Additionally, plates made of carbon fibre reinforced plastics can even make a better use of these states thanks to their strength and elastic behavior, which allows for highly deformed shapes [3]. Modal testing can be an excellent tool for understanding the vibration changes in heated plates in post-buckling. First, it can help in the prediction of buckling, using the Vibration-Correlation Technique (VCT). Second, it can allow the exploration of deep post-buckling states, included those after the occurrence of mode jumping.

VCT technique relies on the principle that, often, a relation between changes in the vibration frequencies and buckling can be established. This relation can allow to obtain reliable estimations for the occurrence of buckling by monitoring the evolution on the frequencies in the loaded structure. VCT has successfully been applied to different kinds of structures, such as columns, plates, and more recently to cylinders. Labans et al. [4] performed vibration correlation studies on conventional laminated cylinders and fibre steering cylinders. VCT was applied by Arbelo et al. [5,6] for the estimation of buckling load of perfect and imperfect flat metallic

* Corresponding author.
E-mail address: c.bisagni@tudelft.nl (C. Bisagni).

https://doi.org/10.1016/j.jsv.2022.117145
Received 28 February 2022; Received in revised form 4 June 2022; Accepted 20 June 2022
Available online 21 June 2022

plates and cylindrical shells. Examples of the VCT method applied to different structures were also reported by Abramovich [7]. On recent studies, the technique has also been successfully applied to grid-stiffened cylindrical shells [8], and to isotropic cylinders with reinforced circular cutouts [9], which suggests that the applicability of the method can be extended to more complex structures.

Even though it is well understood that changes in the vibration signature of plates can be used to predict buckling, it is not known whether a similar procedure can be used to predict their mode jumps. This possibility can, however, be explored via modal testing. A reasonably large amount of studies on the vibration of heated, post-buckled plates is available in literature. The approaches are heterogeneous, since they comprise analytical, numerical and experimental studies, and consider plates made of various materials and under diverse boundary conditions. Chung and Clevenson [10] investigated how acoustic emissions would affect the resonance frequencies and induce mode jumping in stiffened, pre-heated plates; Thompson and Virgin [11] performed experimental studies on the mode jumping in metallic plates subjected to noise and pulses; while Jacobson [12] tested multi-bay, curved and flat composite panels under thermal and high intensity acoustic excitation. More recently, Sun et al. [13] performed an experiment where the mode jumping on heated, acoustically excited C/Si plates were studied. Ehrhardt and Virgin [14] tested heated metallic plates and verified the existence of alternative equilibrium states by using a poking bar as external perturbation source. There are also several numerical studies in plate vibration and mode changes in metallic and composite plates: Kuo [15] performed studies on the changes of vibration patterns after the mode jumping in composite plates; Xia and Xen [16] investigated the vibration of heated post-buckled sandwich plates with functionally graded material facesheets; Chen and Virgin [17] performed dynamic analysis of modal shifting and mode jumping in rectangular, metallic, thermally buckled plates; and Murphy et al. [18] characterized the buckling and snap-through phenomena in heated, fully clamped rectangular plates.

While there seems to be a lot of available research on the application of VCT to mechanically compressed composite structures, there appears to be a gap in the study of the application of VCT to heated composite plates, as well as in the investigation of their frequency changes after a mode jumping has occurred.

During the present investigation, modal testing of rectangular, laminated, heated plates were performed. In these experiments, two plates were tested under both unbuckled and post-buckled states, including the plate configurations reached after a mode jumping. Two goals were pursued: first, the application of VCT technique for the capture of buckling on heated composite plates; second, the investigation of any potential change in the frequency signature of the plates at the moment of the mode jumping. To achieve these objectives, two experimental configurations were used. The main difference between the two setups was the used heat source, being these an oven for the test setup No. 1 and an Infrared (IR) lamp array for the test setup No. 2.

The structure of this paper is here presented. In Section 2, the fundaments of the VCT are briefly explained. In Section 3, the two experimental configurations are described, while the test methodology followed for the execution of the experiments is presented in Section 4. In Sections 5 and 6 the results are reported and evaluated, while Section 7 contains a summary of all obtained results. The conclusions are reported in Section 8.

2. Vibration correlation technique in heated plates: buckling and mode jumping

The vibration correlation technique (VCT) is an experimental, non-destructive technique that allows the prediction of the buckling load in a slender, axially loaded structure. This technique consists on monitoring the variation in the vibration frequencies of the structure with respect to the applied compressive load. Based on the evolution of these frequencies, good estimations of the buckling load can often be obtained by using data acquired at load levels below the 60% of the originally predicted buckling load. This is, therefore, a valuable technique when dealing with structures liable to fail due to buckling. The same principle can also be applied to structures under the effect of thermal loads. In a heated structure, stresses often arise due to restrained thermal expansion, sometimes being large enough to buckle the structure. Such stresses are a function of the coefficients of thermal expansion (CTE), the laminate in-plane and bending stiffness, the boundary conditions and the temperature distributions in the structure [19]. When temperature changes are present, assessing the loads in a structure becomes a difficult task. In those cases, VCT can be a valuable alternative for the estimation of buckling load.

The VCT methodology is rooted on the similarity between the equations for buckling and vibration, investigated early on by Lurie [20,21], and later by Souza et al. [22]. Given the case that a given vibration mode is comparable in shape to the buckling mode, a linear relation between the square of the frequencies and the applied load can often be established. In order to illustrate this concept, a flat,

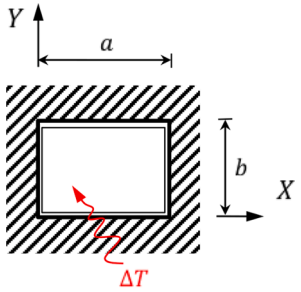

Fig. 1. Plate reference system.

rectangular plate is now considered. The plate is placed in a coordinate system XYZ, and the XY plane coincides with the mid-surface of the plate, with the lower left corner of the plate as the origin of the coordinate system, as shown in Fig. 1. The plate has length a, height b and thickness h, is made of carbon composite material, and has a symmetric and balanced angle-ply layup. The plate is loaded under a uniform temperature increment ΔT, which is applied gradually. Plate length and width variations are constrained, and rotations around the edges are also constrained.

The vibration-buckling behavior of an orthotropic composite plate can be represented by the differential equation reported as Eq. (1):

$$D_{11}w_{,xxxx} + 2(D_{12} + 2D_{66})w_{,xxyy} + D_{22}w_{,yyyy} + \bar{\rho}\ddot{w} = N_x w_{,xx} + N_y w_{,yy} \tag{1}$$

where the comma-preceded sub-indexes represent partial derivatives with respect to the specified variables, and the double dot represents double time derivative; $\bar{\rho}$ represents the equivalent density, calculated as $\bar{\rho} = \sum_{k=1}^{N} \rho_k h_k$, where N is the total amount of stacked layers, and h_k, ρ_k are the height and density of the corresponding layers; the D_{ij} (i, j =1, 2, 6) represent the laminate bending stiffness, and N_x, N_y, N_{xy} are the edge force reactions along X, Y axes. The appearance of thermal loading in Eq. (1) takes place through the membrane constitutive equations:

$$\begin{Bmatrix} N_x \\ N_y \\ N_{xy} \end{Bmatrix} = \begin{bmatrix} A_{11} & A_{12} & 0 \\ A_{12} & A_{22} & 0 \\ 0 & 0 & A_{66} \end{bmatrix} \begin{Bmatrix} \varepsilon^0_{xx} \\ \varepsilon^0_{yy} \\ \gamma^0_{xy} \end{Bmatrix} - \begin{Bmatrix} \widehat{N}^T_x \\ \widehat{N}^T_y \\ \widehat{N}^T_{xy} \end{Bmatrix} \Delta T \tag{2}$$

where the terms A_{ij} (i, j =1, 2, 6) represent the laminate in-plane stiffness, ε^0_{xx}, ε^0_{yy} γ^0_{xy} are the engineering strains, and $\widehat{N}^T_x$, $\widehat{N}^T_y$, $\widehat{N}^T_{xy}$ are the unitary thermal force resultants, which depend uniquely on laminate properties. Thermal forces vanish when $\Delta T = 0$. Eq. (1) captures the interaction effects of thermal and mechanical load over both plate vibration and buckling phenomena.

The typical vibration-buckling behavior of such plate is described in Fig. 2 where two graphs are presented in a stacked form. The upper graph represents the out-of-plane deflections w measured at the plate center versus the applied ΔT, while the lower graph represents the square of the frequencies f^2 versus ΔT. In both graphs, two lines in colour black and blue are plotted, representing the typical behavior of plates without and with geometric imperfections. In order to differentiate buckling shapes from vibration modes, buckling shapes are represented as pairs of integer values between parenthesis such as (m, n), meaning m and n the number of half-waves in X and Y directions, respectively. For plate vibration modes the same notation holds, however the integer pair is between angle brackets, i.e. $\langle m,\ n \rangle$.

Taking now the bold black line for the plate without imperfections at $\Delta T = 0°C$, the plate is under a stress-free state. If temperature increases, in-plane stresses appear in the plate, and the plate remains flat. If temperature keeps increasing, the plate finds a bifurcation

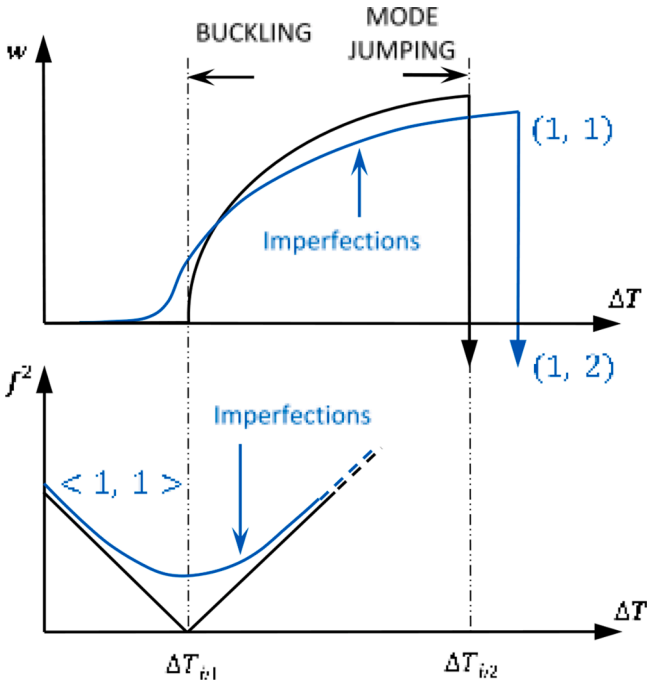

Fig. 2. Behavior of a heated composite plate: Out-of-plane deflection and squared frequency as function of the temperature variation.

point at ΔT_{b1}, beyond which it starts deflecting out-of-plane, typically in a $(1,1)$ buckling shape. This point is known as buckling temperature, represented here as ΔT_{b1}. Meanwhile, in the lower graph, the bold black line represents the vibration mode $\langle 1,\ 1\rangle$ for the plate without imperfections, which is the lowest frequency mode at$\Delta T\ = 0 \circ C$. This vibration mode is also comparable in shape to the previously described $(1,\ 1)$ buckling mode, and is the relevant vibration mode for the application of VCT. At ΔT=0℃, the intersection of the black curve with the vertical axis yields the square of the frequencies of the plate at room temperature. When ΔT increases, f^2 experiences a linear decrease, up to a certain value of ΔT for which f^2 becomes zero, an event that characterizes buckling [23]. This point coincides with the buckling temperature ΔT_{b1}. It constitutes the conceptual basis of the VCT methodology: for the plate without imperfections, when the applied load equals the buckling load, the frequency of the vibration mode, which more closely resembles the buckling shape, is equal to zero.

However, in reality, plates have geometric imperfections and their buckling and vibration behavior deviate from the ideal behavior. Regarding plate deflections, in Fig. 2 it can be seen that plates with geometric imperfections do not show a perfectly defined bifurcation temperature ΔT_{b1}, as the plate deflects gradually, describing a trajectory that asymptotically approaches the deflection curve for the

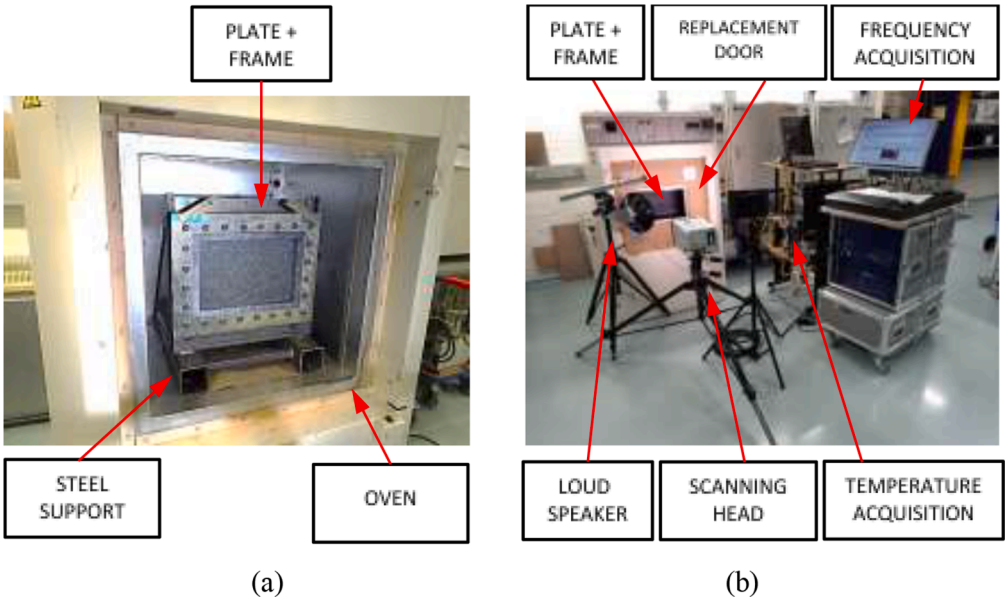

Fig. 3. Test setup No. 1: (a) Details of plate fixture; (b) Complete setup.

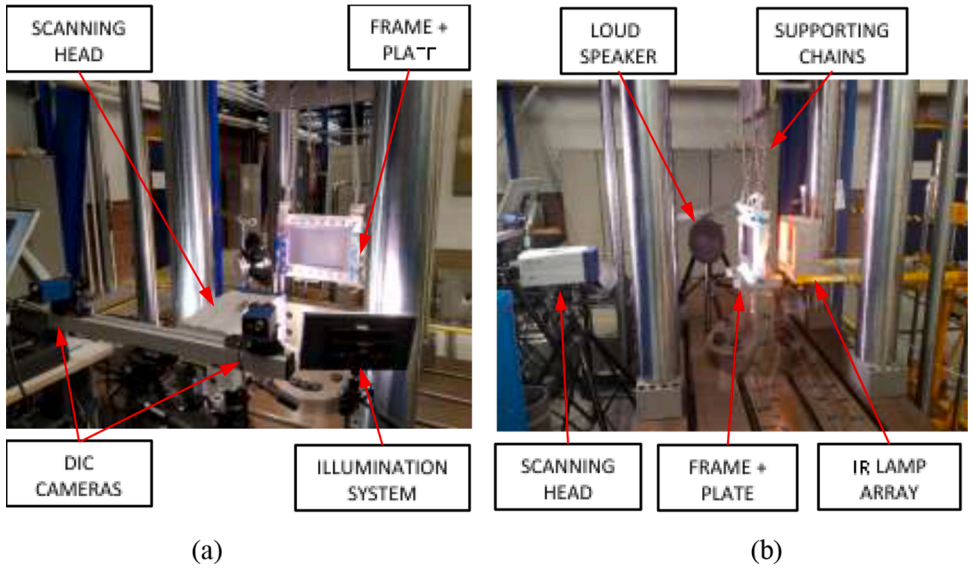

Fig. 4. Test setup No. 2: (a) Front view; (b) Lateral view.

Table 1
Material properties.

	E_{11} [GPa]	E_{22} [GPa]	G_{12} [MPa]	ν_{12}	α_1 [$\mu m/m^{\circ}C$]	α_2 [$\mu m/m^{\circ}C$]	h_{ply} [mm]	ρ [kg/m^3]
AS4 /8552	135	9.68	5.6	0.30	0.28	28	0.181	1.58
Invar 36	140			0.33	1.5			8.05

ideal plate [23]. The presence of geometrical imperfections manifests in the vibration signature of the plate in several ways. First, vibration frequencies for plates with geometric imperfections are inherently higher than for their ideal counterparts. This is illustrated in the lower graph of Fig 2: for ΔT=0℃, the intersection of the blue curve with the vertical axis is slightly higher than for the curve of the ideal plate, and this tendency accentuates as ΔT increases, because the out-of-plane deflections grow larger with the temperature, producing a stiffening effect over the plate [24]. Second, the evolution of f^2 vs. ΔT is not a line anymore, since the linear decrease only holds up to a load level close to buckling. The vibration frequency is not zero at buckling temperature ΔT_{b1}, but instead it reaches a local minimum at approximately the same location. Identifying the local minimum on this curve is a reliable method to identify the buckling load in plates [5]. However, an estimation of the buckling load can be done by performing a linear extrapolation of the linear segment in the f^2 vs. ΔT curve and finding its intersection with the horizontal axis.

When the plate is in post-buckling and the temperature keeps on increasing, the plate can experience a mode jumping, changing the buckling shape from $(1,\ 1)$ into a $(1,\ 2)$ mode. It is difficult to estimate when a mode jumping is going to occur even because VCT is based on plate linear behavior, and the relation between the frequencies and buckled states ends up at the point of buckling.

3. Experimental setups

The present experimental investigation was performed using two different test setups. The first test setup, here called test setup No. 1, was in part based on a previous research by the authors [25], while the second one, here called test setup No. 2, was developed as a novel test configuration. The two test setups are represented in Figs. 3 and 4, respectively.

In both setups the composite plate was fixed within a low CTE frame. The plate and the frame are subjected to heat increments and, due to restrained thermal expansions, the plate experiences buckling and eventually mode jumping. The heating operation is performed gradually, by increasing the temperature in small steps, so that the temperature can stabilize at the desired values, and then the vibration modes and the frequencies can be measured through modal tests.

The tested plates were made of carbon unidirectional composite material. Hints for design of laminates displaying mode jumping under heating can be found in a previous work by the authors [25]. The plates were made of AS4/8552 [26] composite material, and have a stacking orientation of $[30/-30/5/-5]_s$ and $[35/-35/10/-10]_s$. The plies were cut using an automatic cutting machine and were subsequently stacked manually, and the laminate was cured in an autoclave. The frame was constructed using Invar 36 material [27]. The material properties of the composite and the Invar 36 material are presented in Table 1. The low CTE of the frame contributes to restrain the thermal expansion of the plate and to have low sensitivity to thermal gradients in the fixture. Prior to testing, the composite plate was placed between the two parts of the frame and assembled, following a cross sequence to bolt the assembly in three levels up to the maximal level of 60 Nm.

During the modal tests, a POLYTEC PSV 500 XTRA system was used to capture both the vibration frequencies and deflection shapes of the plates at different temperatures. The scanning head of the vibrometer was equipped with a full optics and camera setup with a laser beam, which allowed to perform the calibration and measurements directly from a fully dedicated acquisition and processing unit system. In order to measure the frequency response, the plate and the frame were acoustically excited using a loudspeaker.

The test setup No. 1 is presented in Fig. 3. In this configuration, the assembled plate and frame were placed on top of a metallic support inside an oven, which acted as heating source. The oven can contain specimens up to 600 mm x 600 mm x 600 mm. The oven

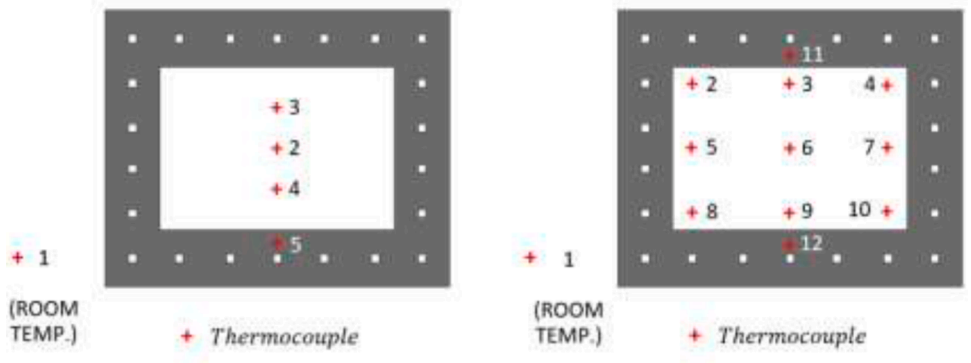

Fig. 5. Thermocouple distribution: (a) Test setup No. 1; (b) Test setup No. 2

door was substituted with a replacement door, which had a rectangular aperture, slightly larger than the plate, so to allow direct access to the measurement devices. In order to close the gap between the frame and the oven door, an aluminum sheet was used. The temperatures on the plate and the frame were monitored using thermocouples, which positions are reported in Fig 5 (a), and thermocouple readings were acquired by a Keythley multimeter. During the experiment, the temperature was increased by manually regulating the temperature in the oven. Due to the test configuration, it was not possible to use both Digital Image Correlation (DIC) and vibrometry at the same time. In this setup, a plate with layup $[30/-30/5/-5]_s$ was tested.

In the test setup No. 2, reported in Fig. 4, the frame was kept suspended in the air with the help of two chains, to recreate as much as possible free-free boundary conditions. For convenience, the test setup was assembled within the working space of a MTS 3500 compression machine. The heating operation was performed using a quartz infrared (IR) lamp array. The temperatures on the plate and frame were monitored using thermocouples, which positions are reported in Fig. 5 (b). A total of nine thermocouples were placed on the plate. The out-of-plane deflections of the plates were measured using a DIC system, using two cameras with 50 mm lenses. The plate tested in this setup had a stacking orientation of $[35/-35/10/-10]_s$.

4. Testing methodology

Due to the differences of the two test setups, the testing protocol had to be slightly different. The test setup No. 1 had the limitation of not being able to capture both DIC deflections and vibration data simultaneously, and consequently the frequency data could not be exactly related to the experimental plate deflections. In order to be able to obtain comparative information, two tests were consecutively performed. During the first test, the plate and the frame were monotonically heated, reaching both buckling and mode jumping, and acquiring DIC deflection shapes and temperatures in the plate. After that, the setup was let to cool down. During the second test, the plate and the frame were subjected to temperature increments. Once the temperature was stabilized, the vibration frequencies were measured, repeating this measurement at different temperatures. The buckling and mode jumping temperatures measured during the second test, together with the deflection shapes acquired during the first test, closely resembled a VCT test. The test setup No. 2 could conveniently fit all the instrumentation around the plate, and therefore DIC and vibration data could be acquired during the same experiment. The plate and the frame were subjected to temperature increments and, once the temperature was stabilized, both DIC and vibration frequencies were measured, repeating these measurements at different temperatures.

Unfortunately, during the tests performed using the two different test setups, the temperature distributions were not homogeneous and consequently the temperature at the centre of the plate was considered as a reference. The frequency measurements were performed using the laser vibrometer and measuring the response to acoustic excitation at each position of an array of points located on the surface of the plate. The scanning head measured the response to the external excitation at each position of the preselected matrix of points. The excitation was performed with a loudspeaker placed in the proximities of the plate. The signal used for excitation with the loudspeaker was an acoustic, "Burst chirp" type signal, sweeping the frequency range of $1-600$ Hz and $1-800$ Hz for test setups 1 and 2, respectively. In the test setup 2, a Hanning window was applied in order to improve measurement coherence. An averaging of three measurements per scanned point was performed.

5. Experimental results for test setup No. 1

For the test setup No. 1, deflections plots are presented in Fig. 6 in two rows, where the plots reported in the upper row represent the buckling, and the plots in the lower row the mode jumping. In the first row it can be appreciated how a $(1,1)$ buckling shape started to be incipient at 56℃. Then, it gradually conformed as the temperature increased, and became fully developed at 76℃. The buckling temperature was extracted graphically by applying the Southwell method [23]. For this, the data for the first test was plotted in a w/ΔT vs. w graph, as shown in Fig. 7. The experimental data points, represented as circles, were fitted to a line, reported as a thin blue line with the label "fitted line". Finally, the buckling temperature was obtained by extracting the inverse of the slope of the fitted line. For this case, it yields a buckling temperature of $T_{b1}(\text{Exp}) = 71C$. Regarding the mode jumping, in the second row of Fig. 6 it can be seen

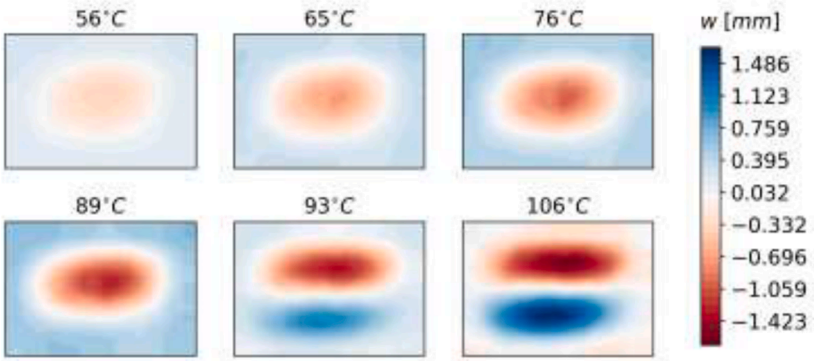

Fig. 6. Out-of-plane displacements **w** for $[30/-30/5/-5]_s$ plate.

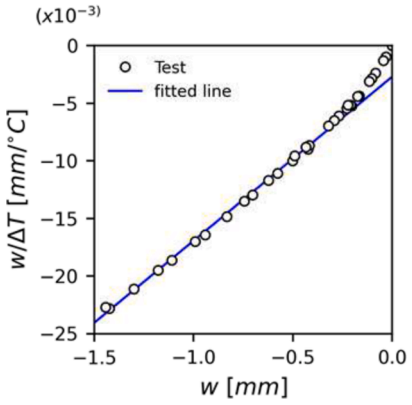

Fig. 7. Southwell plot for $[30/-30/5/-5]_s$ plate.

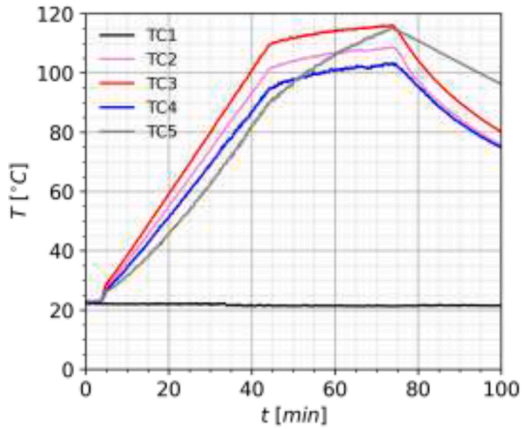

Fig. 8. Thermocouple measurements for $[30/-30/5/-5]_s$ plate.

that at 89℃ the plate still showed a $(1,1)$ buckling shape, being the maximum deflection equal to 1.4 mm. A secondary $(1,2)$ buckling shape appeared at 93℃, being the lower half-wave smaller in size than the upper one. At 106℃, the two half waves became approximately equal in size. The mode jumping temperature $T_{b2}(\text{Exp})$ is considered to have happened around 93℃.

Fig. 8 reports the temperature readings. Temperature differences among the different thermocouple measurements were approximately 10℃ when the reading of TC2 is 60℃, and around 15℃ when the reading of TC2 is 105℃. Such temperature distributions were far from the ideal, uniform temperature distribution which was desired. They were caused by an inherent characteristic of the test setup: air convection flows upwards, and due to this the hotter air concentrated in the upper areas of the oven. Thus, the temperature distribution could not be completely uniform.

In Fig. 9, eight measured frequency spectra are reported. In these graphs, the displacement measured in μm is plotted versus the excitation frequency, measured in Hz. The peaks indicate relevant vibration modes at a given frequency. A black label indicates the first relevant mode, that is $\langle 1,\ 1\rangle$; red and blue labels identify the second and third plate vibration modes, respectively; fourth modes and higher are reported in violet. The lowest measured vibration mode $\langle 1,\ 1\rangle$ in Fig. 9 closely resembles the $(1,1)$ buckling mode displayed by the plate. This vibration mode can be identified in Fig. 9, at the graph acquired at 23℃, as a peak at 215 Hz. First, this vibration mode experienced a decrease in frequency as the temperature increased: for temperatures 33℃, 42℃, 53℃, 67℃, the frequency sank down to the values 188 Hz, 168 Hz, 140 Hz, and 97 Hz, respectively. The lowest frequency value of 94 Hz was measured at approximately 83℃, after which it increased again. The mode $(1,2)$ in red is the mode which resembled the (1,2) post-buckling shape after the mode jumping. It can be seen that this mode is not present between 42℃ and 83℃. Conversely, the mode $\langle 2,1\rangle$ identified in blue is present in all performed modal tests. At room temperature, i.e. at 23℃, it shows a vibration frequency of 416 Hz, gradually decreasing as temperature increases; the frequency for this mode finds a minimum at 67℃, after which it increases again, reaching 511 Hz at 110℃.

In Fig. 10, some examples of vibration shapes are displayed. These were obtained at three different temperature levels, 23℃, 33℃, and 53℃. In the upper row, corresponding to 23℃, the three first captured vibration modes are reported. These were the $\langle 1,\ 1\rangle$, $\langle 2,1\rangle$ and $\langle 1,2\rangle$, with frequencies 215 Hz, 416 Hz and 457 Hz, respectively. The frequency of the first vibration mode $\langle 1,\ 1\rangle$ decreased with the temperature, becoming 187 Hz at 33℃ and 140 Hz at 53℃.The vibration modes $\langle 2,\ 1\rangle$ and $\langle 1,\ 2\rangle$ appeared to experience rotations

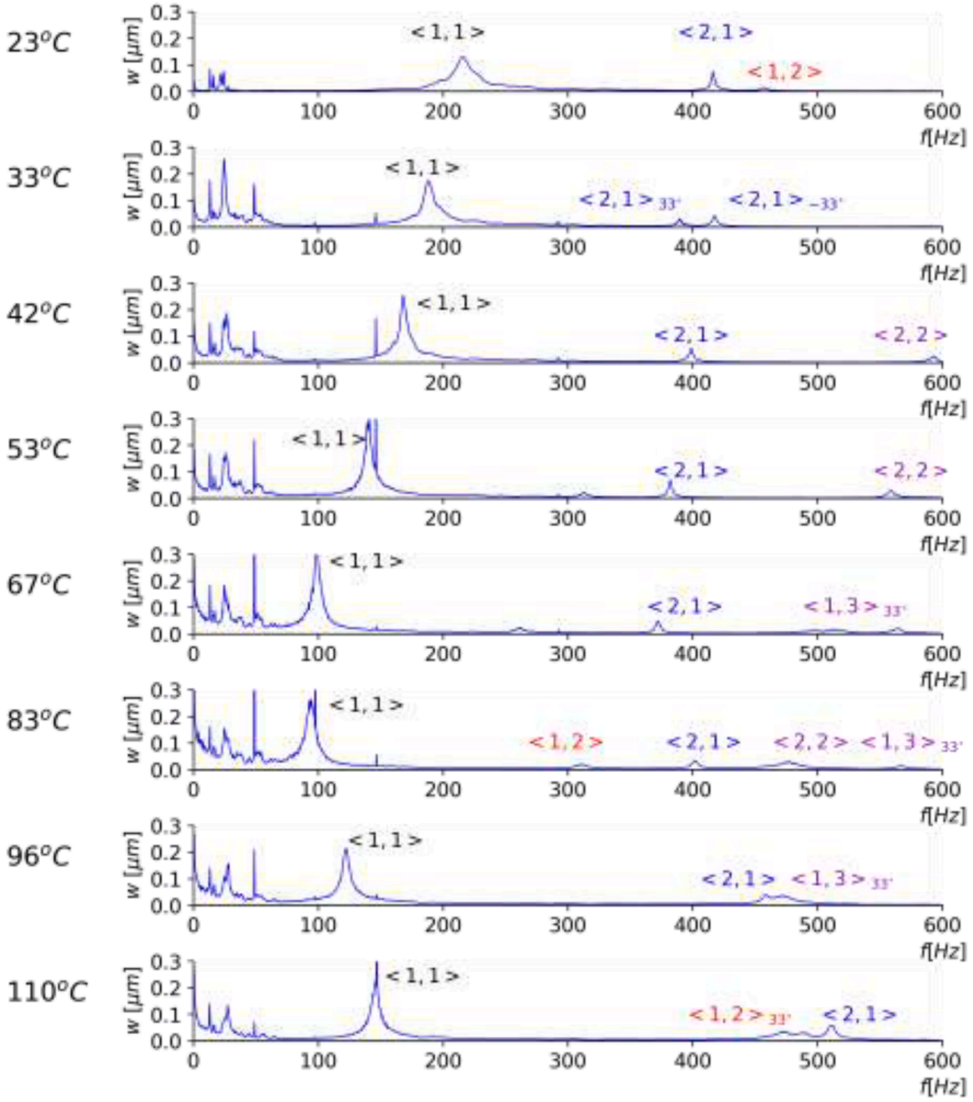

Fig. 9. Frequency spectra for $[30/-30/5/-5]_s$ plate.

of 33° and -33° respectively, as temperature was risen. In order to represent skew or rotated vibration mode shapes, the notation $\langle m, n\rangle_\theta$ was used, where the sub-index θ indicates the angle of rotation of that mode with respect to the X axis. In this way, at T=33°C, the $\langle 2,1\rangle_{33}$ mode shape captured at 389 Hz represents a $\langle 2,\ 1\rangle$ vibration mode shape with two half-waves along the line at θ=33°, approximately the diagonal of the plate connecting the lower left and upper right corners in the plate. Thus, at 33℃ the vibration modes $\langle 2,\ 1\rangle_{33°}$ and $\langle 2,\ 1\rangle_{-33}$ were captured, and they appeared to merge into a $\langle 2,\ 1\rangle$ vibration mode at 53℃.

5.1. Prediction of buckling using VCT

The evolution of the first vibration mode $\langle 1,\ 1\rangle$ is summarized in a graph where f^2 is plotted versus T, reported in Fig. 11(a). A black thin line with "+" markers labelled as "$\langle 1,\ 1\rangle$" represents the measured frequencies for mode $\langle 1,\ 1\rangle$, and the positions of each individual marker represents a single frequency measurement. It can be seen how from 23℃ up to 67℃, the frequency squared f^2 decreased almost linearly and then, after 83℃, it increased again. The first four frequency measurements located in the linear portion of the curve were used to extract a fitted line using the least-square method. This line, represented in the graph as a blue dotted line labelled as "VCT", yields an intersection point with the horizontal axis that can be used as a prediction for the buckling temperature. This prediction value will from now on be referred as $T_{b1}(VCT)$, yielding for this particular case $T_{b1}(VCT) = 75°C$. This prediction can be verified by using the minimum of the f^2 vs T curve, located between the measurements at 67℃ and 83℃. A fitted polynomial curve, represented in the figure as a brown dashed line, was used to extract this minimum. This curve finds a minimum at 77℃, that is, only 2℃ apart from the obtained $T_{b1}(VCT)$. Deflections reported in Fig. 6 indicate that, indeed, the plate has a clear $(1,1)$ buckling shape

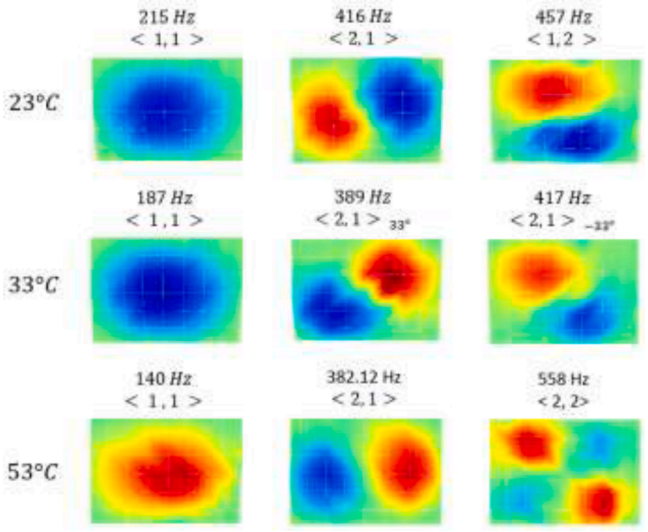

Fig. 10. Examples of vibration mode shapes at various temperatures for test setup No. 1.

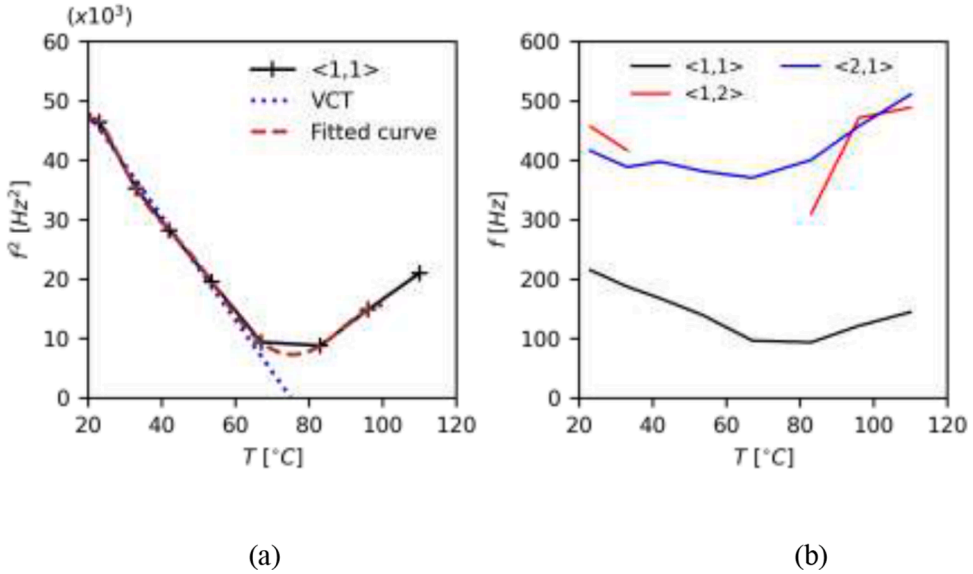

Fig. 11. Frequencies vs. temperature for $[30/-30/5/-5]_s$ plate: (a) Lowest vibration mode; (b) Three lowest vibration modes.

around 65℃ and that this is fully conformed at 75℃. The VCT predicted temperature $T_{b1}(\mathrm{VCT})$ appears therefore to correctly point towards the buckling temperature. It must be noted that determining a precise value for the experimental buckling load in plates is a difficult task, since buckling is a gradual procedure and the out-of-plane deflections increase gradually.

5.2. Detection of the mode jumping

The vibration signature of the plate was then investigated to see if it could be related to the mode jumping. For this, the evolution of modes $\langle 1,1\rangle$, $\langle 2,1\rangle$ and $\langle 1,\ 2\rangle$, which are the first three modes of the plate at room temperature, are shown in Fig. 11 (b), reporting f versus T. While the vibration modes $\langle 1,\ 1\rangle$ and $\langle 2,\ 1\rangle$ could be tracked throughout all temperatures, the mode $\langle 1,\ 2\rangle$ disappeared after 33℃, and did not reappear till 83℃. None of the aforementioned curves showed either maxima or minima at temperatures close to the mode jumping. At temperatures close to the mode jumping there is some overlapping between modes $\langle 1,\ 2\rangle$ and $\langle 2,\ 1\rangle$. Already in Fig. 9 it can be seen how these two modes appear to change their order at frequencies in the [450 −550] Hz range. However, the definition of these modes was insufficiently captured.

The test setup No. 1 presented some issues regarding the acquisition of vibration frequencies. When acoustically excited, not only

the frame and plate but the complete assembly i.e. oven, metallic support, door, etc. vibrated, so the vibration modes originated from the assembly appeared in the measurements. This can be observed in the first graph of Fig. 9, which corresponds to the modal test at 23℃. Most of the frequency readings registered within the frequency band $0-60$ Hz correspond to the vibration of the test hardware, and not only the plate-frame assembly. For this reason, the measurements in this frequency band should be neglected. Additionally, the noise generated by the oven fan introduced an additional excitation in the test setup, so the acoustic signal emitted by the loudspeaker had to be loud enough to overcome it. It is suspected that mode $\langle 1,\ 2\rangle$ and other higher modes could not be accurately captured throughout all temperatures due to lack of resolution in the frequency sampling during acquisition. The vibrometer acquisition unit uses a Fast Fourier Transform (FFT) algorithm, which allows for separation of the plate response into individual frequency components. This procedure requires a discretization of the frequency range of interest, where both the range and the resolution of such discretization parameters have to be selected by the user. Lowering this resolution allows for smaller measuring and processing times, but can yield defects in the measurements such as aliasing or leaking. While the used resolution proved enough to capture the buckling of the plate via VCT, it would appear not to be sufficient to capture the higher modes, $\langle 1,\ 2\rangle$ and $\langle 2,\ 1\rangle$ in detail, where it is believed that potentially valuable information about the mode jumping may be. The lessons learned from this setup were, however, useful for the development of test setup No. 2.

6. Experimental results for test setup No. 2

The out-of-plane deflections measured on $[35/-35/10/-10]_s$ plate using test setup No. 2 are reported in Fig. 12. The three images in the upper row capture the occurrence of buckling, while the bottom row presents the occurrence of the mode jumping. Observing the upper row, it can be seen how at 23°C, that is the room temperature, the plate remained flat, while at 46°C an incipient (1,1) buckling shape can be appreciated, and at 67°C the same shape appeared fully developed. The experimental buckling temperature could not be extracted via the Southwell method since there were not enough measurements for the displacement to apply this method reliably. The buckling temperature was estimated to be $T_{b1}(\text{Exp}) = 50^{\circ}$ C, using the "top-of-the-knee" qualitative method [23]. In the bottom row of Fig. 12, it can be observed that at 90°C the plate presented a fully developed (1,1) buckling shape, while at 102°C the change of mode had already happened, being the bottom half-wave smaller than the one at the top, and later at 113°C a (1,2) buckling shape with two equal half-waves was completely defined. The three plots show how there is no sudden occurrence of the mode change: it happens in a rather gradual transition. In Fig. 12, the temperature labels reported on top of each deflection plot indicate the temperature at the centre of the plate at the time of acquisition. The temperature distribution at each of these six measurements can be found in Fig. 13. These temperature plots were generated using a 2D graphical interpolation of the data acquired by the nine thermocouples distributed on the plate as shown in Fig. 5(b). In each temperature plot in Fig. 13, the position of the sensors is documented with a white cross, with a number indicating the temperature value at the instant of the measurement. At room temperature, the temperature distribution remained relatively uniform, but, as soon as heating started, temperature differences on the plate increased to 10°C at the moment of buckling, and then rose up to 16°C once the (1,1) buckling shape was completely developed. The differences in the temperature distributions became more relevant at higher temperatures, as the temperature differences within the plate increased up to 32°C. From the six temperature plots, it becomes evident how the upper part of the plate was hotter, which is consistent with the data registered for the test setup No. 1. Achieving uniform temperature distribution was proven to be a difficult task, and a consistent issue in all performed experiments. It was learned that, in order to avoid air convection problems, the specimen should have been placed in horizontal, being heated from below. Unfortunately, this could not be done due to the additional difficulties this arrangement would bring, such as issues with the wiring of sensors, acquisition instrumentation, and assuring a reliable calibration for the DIC cameras.

The frequency spectra obtained from the modal tests in test setup No. 2 are summarized in Fig. 14. Almost the totality of the noise in the frequency band $0-60$ Hz which was present in the frequency measurements for test setup No. 1 is not present anymore, thanks to the implemented free-free boundary conditions. The evolution of the three vibration modes, $\langle 1,\ 1\rangle$, $\langle 1,\ 2\rangle$ and $\langle 2,\ 1\rangle$, could successfully be tracked throughout all temperature values, and also higher frequency modes were tracked. For the presentation of the

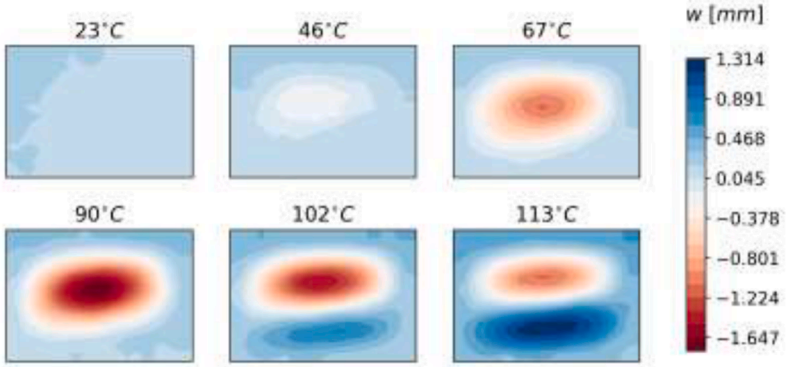

Fig. 12. Out-of-plane displacements w for $[35/-35/10/-10]_s$ plate.

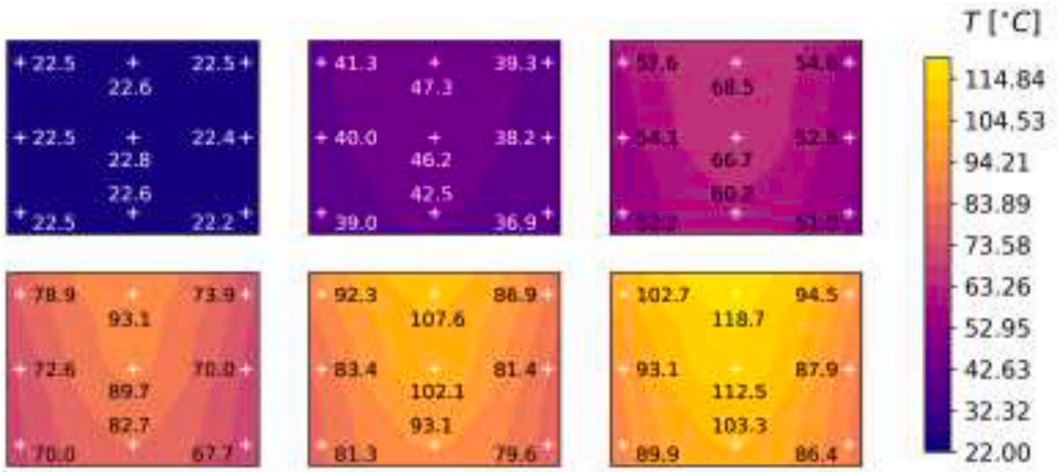

Fig. 13. Temperature distributions for $[35/-35/10/-10]_s$ plate.

frequency measurements, it was found convenient to display the spectra in terms of vibration speed in μm/s.

6.1. Prediction of buckling using VCT

In the top graph in Fig. 14 it can be seen how at room temperature, i.e. 23°C, the lowest vibration mode had a $\langle 1,\ 1\rangle$ shape. Also the buckling shape of the plate was a $(1,\ 1)$ mode. The vibration frequency of mode $\langle 1,\ 1\rangle$ decreased as temperature increased, as it can be seen in the spectra for temperatures 31°C, 36°C, 41°C and 46°C. This evolution can be better appreciated in the plot in Fig. 15(a), where an overview of the variations in f^2 vs T is reported. The variation in frequencies of mode $\langle 1,\ 1\rangle$ is represented as a black thin line with "+" markers labeled as "$\langle 1,\ 1\rangle$", where each "+" indicates a frequency measurement. In the temperature range going from 23°C to 46°C, the value of f^2 for mode $\langle 1,\ 1\rangle$ appears to have a linear decrease. After that, it started to grow, rising up to a local maximum at 67°C, remaining stable till 83°C, after which it rapidly decreased, finding another local minimum at 102°C. The frequency measurements within 23°C to 46°C range were used to extract a fitted line using the least-square method, represented in Fig. 15(a) as black dotted line, labelled as "VCT". The intersection of this line with the horizontal axis yields a $T_{b1}(\mathrm{VCT}) = 58^{\circ}$ C. In order to find an approximate minimum reached by the f^2 vs T curve, a fitted curve was performed using the measurements within the temperature range 23°C to 67°C. This curve is represented as a dashed, brown line with the label "fitted curve", which finds a minimum at 51°C. This temperature has a difference of 7°C with the VCT predicted temperature. It is believed that such difference could be originated by the lack of frequency measurements in the temperature range 51°C - 67°C. The occurrence of buckling in this temperature range is also confirmed by the two deflection plots in Fig. 12 at 46°C and 67°C. VCT appears therefore to correctly hint towards the occurrence of buckling.

6.2. Detection of the mode jumping

An attempt was made to identify relevant changes in the plate vibration frequencies related to the mode jumping. In the second row of DIC measurements reported in Fig. 12, a change from the buckling mode (1,1) into mode (1,2) is clearly observable, happening this between 90°C and 102°C. However, this change did not happen as a sudden event, but as a gradual transition. The evolution of three vibration modes $\langle 1,\ 1\rangle$, $\langle 2, 1\rangle$ and $\langle 1, 2\rangle_{45^{\circ}}$ is shown in Fig. 15 (b). The mode $\langle 2,1\rangle$, reported as a blue curve, is the second mode present at room temperature, with a frequency of 350 Hz. When temperature increased, the frequency for this mode showed a gradual decrease, finding a minimum value of the frequency of 313 Hz at T=51°C. Then, it experienced an increase up to 113°C, where it reached a value of 433 Hz. The curve minimum for this mode appeared to happen at roughly the same temperature as the reported curve minimum for mode $\langle 1,1\rangle$. The third vibration mode present at room temperature was the $\langle 1, 2\rangle_{45^{\circ}}$ mode at 411 Hz. The evolution of this mode is represented in Fig. 15(b) as a bold red curve. When temperature increased, this mode experienced at first a gradual decrease, intersecting the line for mode $\langle 2, 1\rangle$ and becoming the second vibration mode of the plate at a point between the measurements at 51°C and 67°C . This occurred at approximately 58°C, that is shortly after the plate had buckled. After that, the frequency of mode started to increase rapidly, intersecting again the curve for $\langle 1, 2\rangle_{45^{\circ}}$ at around 96°C and thus becoming again the third vibration mode. This second intersection happened somewhere between the measurements at 91℃ and 102℃, approximately at a distance of 5°C to the occurrence of the mode change.

Besides the three examined vibration modes, several occurrences in higher frequency modes were observed during the mode transition. Vibration mode $\langle 2, 2\rangle_{45^{\circ}}$ was present at 83℃ i.e. right before the mode change, and during the buckling mode transition this mode appeared to rotate and become a $\langle 2, 2\rangle$ mode, at 102℃. Additionally, some other higher frequency vibration shapes, such as $\langle 1, 3\rangle_{(33^{\circ})}$ and $\langle 1, 3\rangle_{(33^{\circ})}$, were also captured before the mode change. It should be also commented that beyond 41℃ the measured

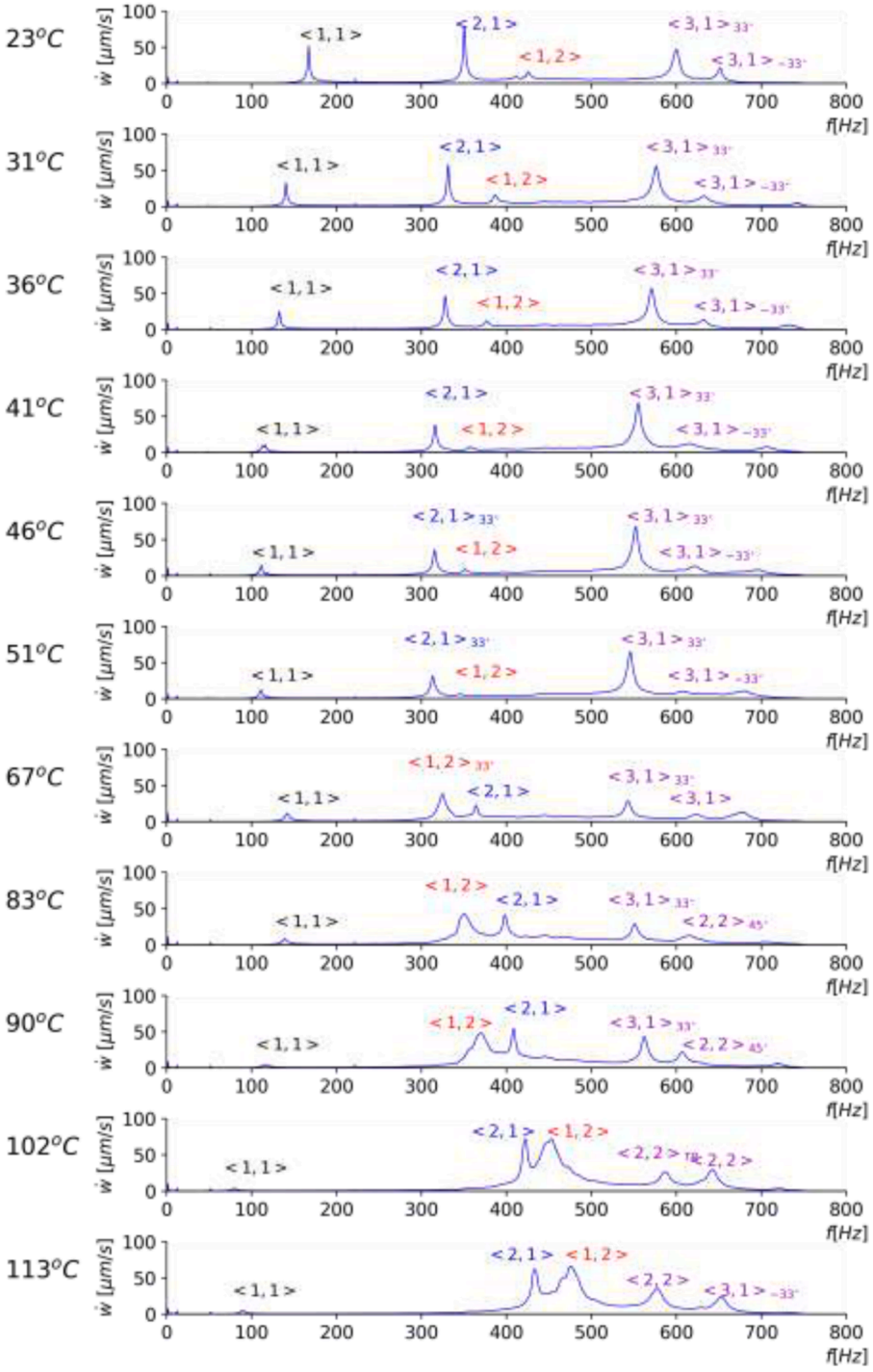

Fig. 14. Frequency spectra for $[35/-35/10/-10]_s$ plate.

speeds decrease significantly for the lowest frequency mode $\langle 1,1 \rangle$, while vibration responses for modes $\langle 1,2 \rangle_{45^\circ}$ and $\langle 2,1 \rangle$ become more relevant as temperature increases beyond 67°C. The significance of previously described events is unclear, and their relation with the mode jumping is found not yet conclusive.

For the experiments performed in test setup No. 1 and test setup No. 2, VCT achieved reasonable predictions for the buckling temperature. This was done by performing a linear extrapolation of the linear part of the f^2 vs T curve and extracting the intersection of the resulting line with the horizontal axis. The accuracy of these predictions could be verified with the minimum in the f^2 vs T curve present in the proximity of buckling. Based on these results, the VCT could be a useful tool for the prediction of buckling in heated

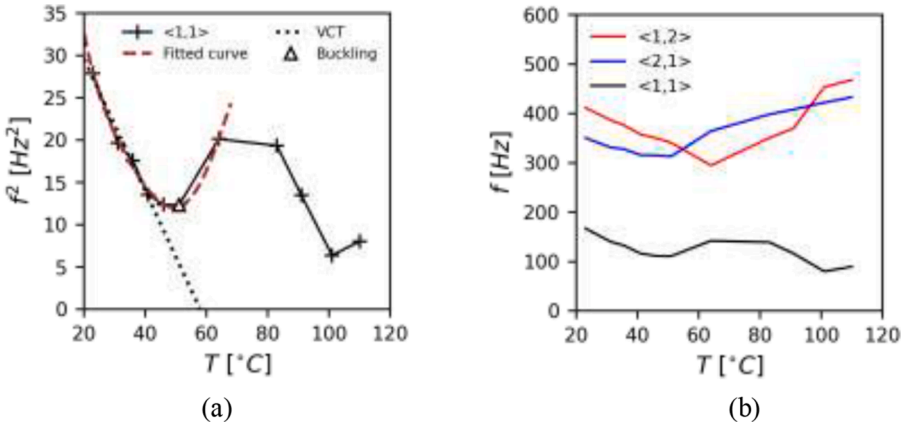

Fig. 15. Frequencies vs. temperature for $[35/-35/10/-10]_s$ plate: (a) Lowest vibration mode; (b) Three lowest vibration modes.

composite plates. Events such as the inversion in order for the modes $\langle\ 1,\ 2\ \rangle_{45}$ and $\langle\ 2,\ 1\rangle$ were detected in the proximity of the mode jumping. However, the relation between such events and the occurrence of the mode jumping is not yet conclusive and requires a further experimental effort.

7. Results summary

In this section, an overview of the main results of this investigation is presented. Table 2 synthesizes the results for the prediction of thermal buckling temperature with VCT, and Table 3 contains the most relevant observations for the mode jumping. For comparison, theoretical values for the buckling and mode jumping temperatures were also reported in the tables. These theoretical values were extracted from Finite Element numerical simulations performed in Abaqus, reported in previous work by the authors [25]. The FE model was performed using S4R shell elements. These are general-purpose Finite Elements, which formulation is based on Koiter-Sanders shell theory. This theory proposes simplifications on the shell kinematic equations which somewhat limits its applicability to moderately large deflections [28]. The theoretical buckling temperature is represented as $T_{b1}(Th)$, and is the result of an eigenvalue analysis, while the theoretical mode jumping temperature, represented as $T_{b2}(Th)$, was obtained by means of a nonlinear dynamic explicit simulation.

7.1. VCT buckling prediction

In Table 2 it can be seen how, for the test setup No. 1, the theoretical prediction $T_{b1}(Th)$ matched well with the obtained experimental buckling temperature $T_{b1}(Exp)$, showing only 3°C difference. On the other hand, the VCT prediction $T_{b1}(VCT)$ appears to have overestimated $T_{b1}(Exp)$ in 4°C. This is yet considered to be a fairly close prediction of the onset of buckling. For the test setup No. 2, the experimental buckling temperature was considerably lower than the theoretical one, with 28°C difference between the two. Despite this difference, VCT delivered a fair prediction of the experimental buckling temperature, with a difference of 7°C between the two. For both test setups the VCT prediction is not on the conservative side since $T_{b1}(VCT)$ is larger than $T_{b1}(Exp)$. In Table 2, the difference in buckling temperatures percent values are calculated with respect to initial temperature 23°C.

7.2. Observations about mode jumping

In Table 3, it can be seen how, for the two test setups, the theoretical prediction for the mode jumping temperature $T_{b2}(Th)$ is higher than experimentally obtained mode jumping temperature $T_{b2}(Exp)$. The differences between them were of 9°C for the $[30/-30/5/-5]_s$ plate and 35°C for the $[35/-35/10/-10]_s$ plate. In the last column of the table, the most relevant interactions in the higher modes are reported. However, there is no conclusive evidence about a relation between these observations and the mode jumping.

Large differences between the theoretical and experimental values for buckling and mode jumping could have been by multiple

Table 2
VCT buckling predictions.

Test setup	Layup	Buckling temperature [°C]			
		$T_{b1}(Th)$	$T_{b1}(Exp)$	$T_{b1}(VCT)$	difference
No.1	$[30/-30/5/-5]_s$	68	71	75	8.3%
No.2	$[35/-35/10/-10]_s$	79	51	58	25%

Table 3
Observations at mode jumping.

Test setup	Layup	Mode jumping temperature [°C]		
		T_{b2}(Th)	T_{b2}(Exp)	Observations
No.1	$[30/-30/5/-5]_s$	102	93	Switching of $\langle 1,2\rangle$ and $\langle 2,1\rangle$ modes.
No.2	$[35/-35/10/-10]_s$	137	102	Switching of $\langle 1,2\rangle$ and $\langle 2,1\rangle$ modes and 45° rotation of mode $\langle 2,2\rangle_{45°}$

factors, such as irregularity in the temperature distributions, changes in material properties due to sustained heating, or other particularities of the test setup.

8. Conclusions

In this investigation, experiments on heated composite laminated plates were performed. Two goals were pursued: first, the application of the Vibration Correlation Technique (VCT) to detect buckling in heated composite plates; second, an exploratory measurement of the vibration frequencies of the composite plates in the proximities of a mode jumping. To this aim, two symmetric and balanced, angle ply laminates with stacking orientations $[30/-30/5/-5]_s$ and $[35/-35/10/-10]_s$, made in material AS4/8552, were tested. The plates were placed inside a frame with a low thermal expansion coefficient, and two different experimental configurations were implemented, using as heat source an oven and an infra-red quartz lamp array, respectively. The plates showed a linear decrease in the square of the frequencies f^2 with respect to the temperature T, and VCT achieved reasonable predictions for the buckling temperature by performing a linear extrapolation of the linear part of the f^2 vs T curve and extracting its intersection with the horizontal axis. The accuracy of these predictions was compared with the experimentally obtained buckling temperature. For the test setup No. 1, VCT prediction overestimated the buckling temperature of only 4°C, while for the test setup No. 2 this difference rose up to 7°C. Regarding the mode jumping, changes in the vibration signature of the plates in the proximities of the mode jumping were tracked. It was found that the f vs T curves for the 2nd and 3rd modes intersected roughly around the temperatures at which the mode change happened. Besides, higher modes experienced a rotation. The relation of these events with the mode jumping is, however, not yet conclusive and further experimental work is required. The main contribution of this work is to show qualitatively and quantitatively the value of the VCT method for the prediction of the buckling temperature of composite plates, as well as the change of buckling and vibration mode.

CRediT authorship contribution statement

J.G. Álvarez: Conceptualization, Methodology, Software, Validation, Formal analysis, Investigation, Data curation, Writing – original draft, Writing – review & editing, Visualization, Project administration. **Haim Abramovich:** Conceptualization, Methodology, Writing – review & editing, Supervision. **Chiara Bisagni:** Conceptualization, Methodology, Resources, Writing – review & editing, Supervision, Project administration, Funding acquisition.

Declaration of Competing Interest

The authors declare that they have no known competing financial interests or personal relationships that could have appeared to influence the work reported in this paper.

References

[1] C.R. Bowen, R. Butler, R. Jervis, H.A. Kim, A.I.T. Salo, Morphing and shape control using unsymmetrical composites, J. Intell. Mater. Syst. Struct. 18 (2007) 89–98, https://doi.org/10.1177/1045389×07064459.
[2] J.G. Álvarez, C. Bisagni, Investigation on buckling and mode jumping of composite plates under thermomechanical loads, Int. J. Non Linear Mech. (2021), 103837, https://doi.org/10.1016/j.ijnonlinmec.2021.103837.
[3] L. Culliford, R.S. Choudhry, R. Butler, A. Rhead, Buckling and strength analysis of panels with discrete stiffness tailoring, Compos. Struct. 234 (2020), 111672, https://doi.org/10.1016/j.compstruct.2019.111672.
[4] E. Labans, H. Abramovich, C. Bisagni, An experimental vibration-buckling investigation on classical and variable angle tow composite shells under axial compression, J. Sound Vib. 449 (2019) 315–329, https://doi.org/10.1016/j.jsv.2019.02.034.
[5] M.A. Arbelo, S.F.M. De Almeida, M.V. Donadon, S.R. Rett, R. Degenhardt, S.G.P. Castro, K. Kalnins, O. Ozoliņš, Vibration correlation technique for the estimation of real boundary conditions and buckling load of unstiffened plates and cylindrical shells, Thin Walled Struct. 79 (2014) 119–128, https://doi.org/10.1016/j.tws.2014.02.006.
[6] M.A. Arbelo, K. Kalnins, O. Ozolins, E. Skukis, S.G.P. Castro, R. Degenhardt, Experimental and numerical estimation of buckling load on unstiffened cylindrical shells using a vibration correlation technique, Thin Walled Struct. 94 (2015) 273–279, https://doi.org/10.1016/j.tws.2015.04.024.
[7] H. Abramovich, The vibration correlation technique - a reliable nondestructive method to predict buckling loads of thin walled structures, Thin Walled Struct. 159 (2021) 107308, https://doi.org/10.1016/j.tws.220.107308.
[8] D. Shahgholian-Ghahfarokhi, G. Rahimi, Buckling load prediction of grid-stiffened composite cylindrical shells using the vibration correlation technique, Compos. Sci. Technol. 167 (2018) 470–481, https://doi.org/10.1016/j.compscitech.2018.08.046.

[9] E. Skukis, O. Ozolins, J. Andersons, K. Kalnins, M.A. Arbelo, Applicability of the vibration correlation technique for estimation of the buckling load in axial compression of cylindrical isotropic shells with and without circular cutouts, Shock Vib. (2017), https://doi.org/10.1155/2017/2983747.
[10] F.N. Chung, S.A. Clevenson, High intensity acoustic tests of a thermally stressed aluminum plate in TAFA, NASA Tech. Memo 101552 (1989).
[11] J.M.T. Thompson, L.N. Virgin, Predicting a jump to resonance using transient maps and beats, Int. J. Non Linear Mech. 21 (1986) 205–216, https://doi.org/10.1016/0020-7462(86)90004-1.
[12] M.J. Jacobson, Sonic fatigue of advanced composite panels in thermal environments, J. Aircraft 20 (1983) 282–288, https://doi.org/10.2514/3.44865.
[13] Y. Sun, Z. Liu, J. Sun, F. Ren, H. Cheng, L. Dong, Snap-through response of thermally buckled C/SiC plates considering boundary elasticity and initial imperfections under progressive wave loading, Compos. Struct. 276 (2021), 114443, https://doi.org/10.1016/j.compstruct.2021.114443.
[14] D.A. Ehrhardt, L.N. Virgin, Experiments on the thermal post-buckling of panels, including localized heating, J. Sound Vib. 439 (2019) 300–309, https://doi.org/10.1016/j.jsv.2018.08.043.
[15] S.Y. Kuo, L.C. Shiau, J.W. Chuang, C.C. Cheng, The relationship of buckle pattern change and vibration mode shifting: Thermal postbuckling and vibration of composite laminates, J. Aeronaut. Astronaut. Aviat. 48 (2016) 65–74, https://doi.org/10.6125/15-1120-869.
[16] X.K. Xia, H.S. Shen, Vibration of post-buckled sandwich plates with FGM face sheets in a thermal environment, J. Sound Vib. 314 (2008) 254–274, https://doi.org/10.1016/j.jsv.2008.01.019.
[17] H. Chen, L.N. Virgin, Dynamic analysis of modal shifting and mode jumping in thermally buckled plates, J. Sound Vib. 278 (2004) 233–256, https://doi.org/10.1016/j.jsv.2003.10.054.
[18] K.D. Murphy, L.N. Virgin, S.A. Rizzi, Characterizing the dynamic response of a thermally loaded, acoustically excited plate, J. Sound Vib. 196 (1996) 635–658, https://doi.org/10.1006/jsvi.1996.0506.
[19] J. Gutiérrez Álvarez, C. Bisagni, Closed-form solutions for thermomechanical buckling of orthotropic composite plates, Compos. Struct. 233 (2020), 111622, https://doi.org/10.1016/j.compstruct.2019.111622.
[20] H. Lurie, Effective end restraint of columns by frequency measurements, J. Aeronaut. Sci. 18 (1951) 566–567, https://doi.org/10.2514/8.2038.
[21] H. Lurie, Lateral vibrations as related to structural stability, J. Appl. Mech. 19 (1952) 195–204, https://doi.org/10.1115/1.4010446.
[22] M.A. Souza, L.M.B. Assaid, A new technique for the prediction of buckling loads from nondestructive vibration tests, Exp. Mech. 31 (1991) 93–97, https://doi.org/10.1007/BF02327558.
[23] J. Singer, J. Arbocz, T. Weller, Buckling Experiments: Experimental Methods in Buckling of Thin-Walled Structures, John Wiley & Sons, Inc., Hoboken, NJ, USA, 2002, https://doi.org/10.1002/9780470172995.
[24] D. Hui, Effects of geometric imperfections on frequency-load interaction of biaxially compressed antisymmetric angle ply rectangular plates, J. Appl. Mech. 52 (1985) 155–162, https://doi.org/10.1115/1.3168987.
[25] J. Gutiérrez Álvarez, C. Bisagni, A study on thermal buckling and mode jumping of metallic and composite plates, Aerosp. 8 (2021) 56, https://doi.org/10.3390/aerospace8020056.
[26] Hexcel Corporation, HexPly 8552, Prod. Data Sheet. (2016), 1-6.
[27] Re-Steel, Invar 36 for composite Tooling data sheet. https://re-steel.com/invar-plate/invar-36/, 2003 (accessed 1 January 2022).
[28] J.L. Sanders, Nonlinear theories for thin shells, Q. Appl. Math. XXI (1963) 21–36. https://www.ams.org/journals/qam/1963-21-01/S0033-569X-1963-0147023-4/.